Crustal Deformation of the Mud Stone Area in SW Taiwan Using the Geodetic Data from 2002 to 2010

Shu-Chin Hsu[*1], Kuo-En Ching[2]
[1]Graduate Student, Department of Geomatics, National Cheng Kung University
1 University Rd., Tainan 70101, Taiwan; Tel: +886-6-2757575#63840
Email: monica198574@yahoo.com.tw

[2]Assistant Professor, Department of Geomatics, National Cheng Kung University
1 University Rd., Tainan 70101, Taiwan; Tel: +886-6-2757575#63840
Email:jingkuen@mail.ncku.edu.tw

KEY WORDS: GPS, precise leveling measurement, Hsiaokangshan fault, creeping fault, earthquake potential

ABSTRACT: The previous geodetic study results of the Parkfield segment of the San Andreas fault in California and the Chihshang fault in eastern Taiwan indicate that the creeping fault still has the potential to generate large earthquakes. High strain rate of ~1.0 μstrain/yr in mud stone area in SW Taiwan shown by previous geodetic data may imply high earthquake potential. However, the historical earthquake records represent no significant earthquakes occurred in this area since 1900. In this study, we therefore mainly adopted the measurements from 201 campaign-mode GPS stations and 2 nearly E-W-trending precise leveling routes to estimate the characteristics of main faults (the Chishang fault and Hsiaokangshan fault) and their earthquake potentials in the mud stone area in SW Taiwan. Similar elevation change patterns of six repeated leveling surveys between 2002 and 2010 from these two routes imply that the vertical deformation rate in this area is stable. The leveling vertical velocities west of the Hsiaokangshan fault are almost zero while the velocities east of the Hsiaokangshan fault rapidly increases to 15-20 mm/yr. Then the rates rapidly decrease to almost no vertical motion. The GPS horizontal velocity field from 2002 to 2010 shows ~60 mm/yr, N267° east of the Chishan fault. Then the horizontal velocities west of the Chishan fault gradually decrease westward to ~11 mm/yr, N264°. Comparing the horizontal and vertical velocity patterns, we notice that the obvious velocity gradient is shown in the area between the Hsiaokanshan and the Chishan fault. Due to the major faults in Taiwan mainly dipping to the west, we preliminarily propose that the high strain rate in mud stone area in SW Taiwan results from the motion of the Hsiaokanshan fault. In the future, we will use the 2D fault model to evaluate the fault parameters and to estimate the seismic potential in this area.

1. INTRODUCTION

According to the historical records, Taiwan has been experienced over ten destructive earthquakes since last century (e.g., Bonilla, 1977; Cheng and Yeh, 1989), including the 1946 Hsinhua earthquake, the 1964 Baihe earthquake, the 1999 Chi-Chi earthquake, and the 2003 Chihshang earthquake. More than 6000 of people dead during those events indicate that people's life and property in Taiwan are seriously threatened by the sufficiently frequent earthquakes. However, the movement of fault does not always generate earthquake, such as the movement of creeping fault which has been considered as almost no earthquake potential. The previous geodetic study results of the Parkfield segment of the San Andreas fault in California and the Chihshang fault in eastern Taiwan indicate that the creeping fault still has the potential to generate large earthquakes. In addition, because the origin time, location, and magnitude of an earthquake are difficult to be predicted, the probability estimate for the generation of an earthquake in terms of the historical earthquake records and geodetic data becomes an important topic now. The case of the 2010 M_w 8.8 Chili earthquake shows us that the area with seldom earthquakes usually accumulates high seismic strain. While an earthquake occurs, it would result in serious disaster.
Therefore our research used 201 GPS observations and leveling measurements from two routes which across the study area to analyze the earthquake potential and the characteristics of the major faults in the mud stone area of SW Taiwan.

2. TECTONIC SETTING

Taiwan is the product of the convergence between the Eurasian Plate and the Philippine Sea Plate (PSP). The PSP moves northwestward relative to the continental margin (Penghu Islands) with a rate of ~82 mm/yr (Yu *et al.,* 1997). Our study area mainly consists of mud stone in SW Taiwan (Huang *et al.,* 2004). The Hsiaokangshan fault (HKSF) and Chishan fault (CHNF) are two major active faults in this area. The Hsiaokangshan fault which is represented as an obvious fault scarp is located along the western bound of the Takangshan and Hsiaokangshan. The previous seismic study indicates that the Hsiaokangshan fault is an east-dipping thrust fault. The formation of the fault scarp

between Hsiaokangshan and Alien implies that this fault might be still an active fault. The NE-trending Chishan fault is a high-angle sinistral reverse fault.

3. DATA AND METHOD

3.1 GPS

We used GPS observations from 128 GPS stations installed by the Central Geological Survey (CGS) and 73 GPS stations established by the Ministry of Interior (MOI) (Figure 1). A ~5 km dense station-spacing GPS network, containing the 71 campaign-mode and 1 continuous GPS stations was deployed by the CGS since 1995. In order to increase the station density of the GPS monitoring network, the CGS then continued installing 17 GPS stations in 1999 and 20 GPS stations in 2003.

Our research used the software Bernese v.5.0 to calculate the GPS coordinates. The standard deviations of all stations are ~2-5 mm in horizontal component and ~10-20 mm in vertical component.

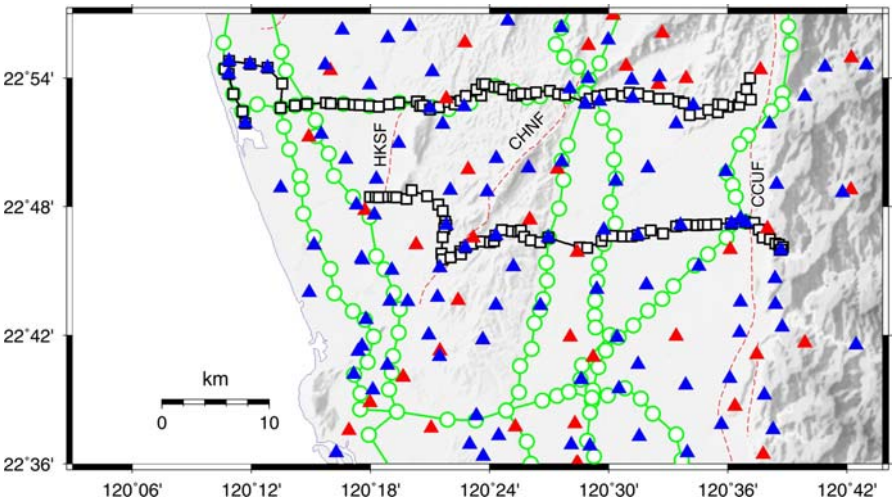

Figure 1. Distribution of the stations used in this study. Blue triangles are GPS campaign-mode stations installed by the CGS. Red triangles are GPS campaign-mode stations installed by the MOI. Green circles are first order first class and first order second class leveling routes installed by the MOI. Black squares are the leveling routes installed by the CGS. Red dashed lines denote the locations of the active faults published by the CGS. HKSF: the Hsiaokangshan fault, CHNF: the Chinshan fault, CCUF: the Chaochou fault.

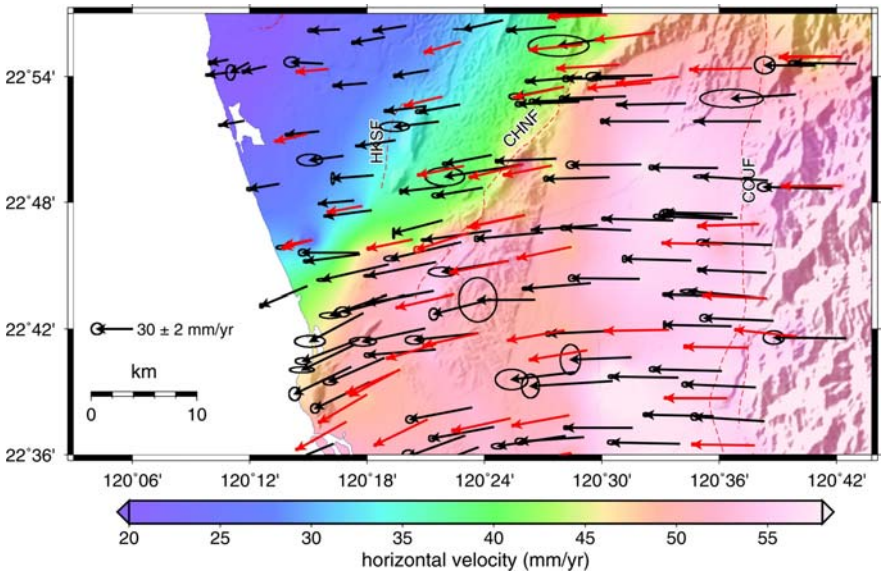

Figure 2. GPS horizontal velocity field relative to the station S01R. Arrows denote the vectors derived by campaign-mode GPS observations. Ellipses at the tips of vectors are the 95% confidence interval. Black arrows are velocities derived from the CGS, while red ones are inferred from the MOI. Red dashed lines denote the locations of the active faults published by the CGS. HKSF: the Hsiaokangshan fault, CHNF: the Chinshan fault, CCUF: the Chaochou fault.

3.2 Leveling Measurement

The leveling data were collected by DiNi12 digital leveling instrument. We mainly adopted leveling measurements from 2 leveling lines. First one is 91 km in length across the northern edge of the Takangshan. This leveling line was repeatedly surveyed 6 times from 2004 to 2010. The other one is 50 km in length across the southern bound of the Takangshan. This leveling line was repeatedly surveyed 7 times from 2002 to 2010. The similar patterns of elevation changes between adjacent two years for the leveling data from these two routes represent the surface deformation is quite stable. We then could calculate the uplift rate of each benchmark by using the least squares method.

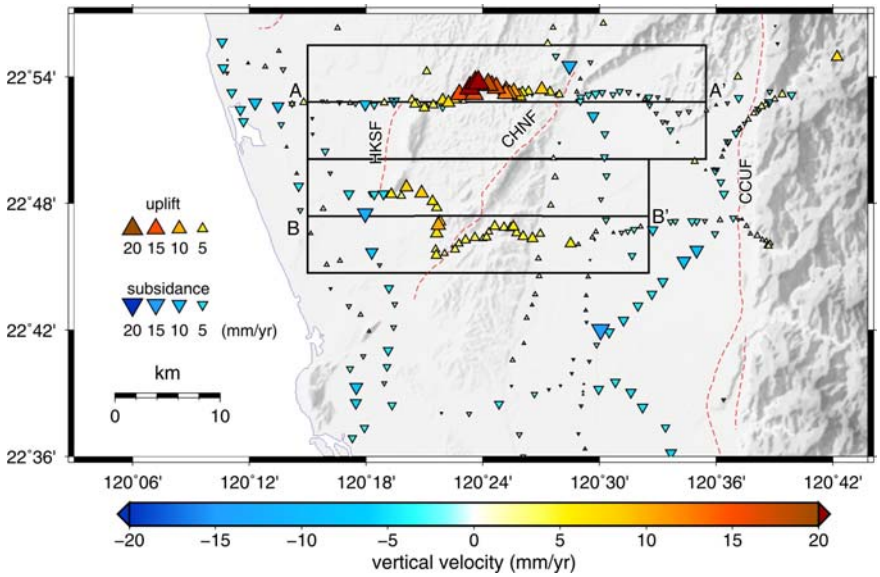

Figure 3. Leveling vertical velocity field relative to the station S01R. Warm-colored triangles denote uplift; while cool-colored inverse triangles represent subsidence. Black squares indicate the locations of velocity profiles. Red dashed lines denote the locations of the active faults published by the CGS. HKSF: the Hsiaokangshan fault, CHNF: the Chinshan fault, CCUF: the Chaochou fault.

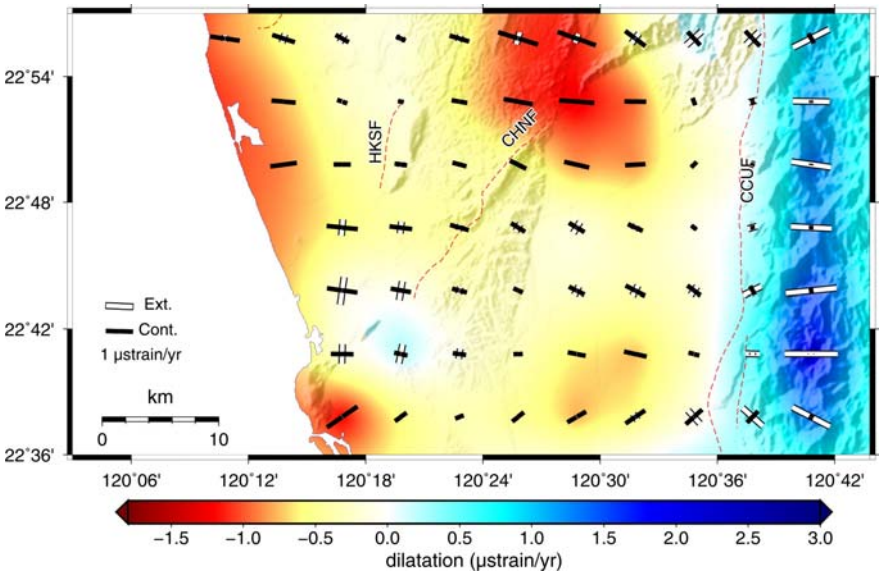

Figure 4. Horizontal dilatation strain rates with the principal strain axes. The thick bars reflect the amount and direction of principal strain rates. The color scale shows magnitudes of dilatation rates. Positive means extension while negative means contraction.

3.3 Strain Rate Field

The strain rate indicates the velocity gradient between the stations, so we evaluated the strain rate according to the GPS horizontal velocities to analyze the spatial characteristics of crustal deformation in the study area (Prescott *et al.,* 1979). The dilatation rate can be considered as a measure of the horizontal deformation related to dip-slip

faulting (i.e., reverse faulting or normal faulting). The rotation rate is derived from the asymmetric portion of the velocity gradient tensor and the positive rotation rate is considered to be a clockwise rotation.

3.4 GPS Profile

To investigate the activities of the Hsiaokangshan fault and Chishan fault, we decomposed horizontal velocities into the fault-parallel and fault-perpendicular components along two velocity profiles to characterize the movement behaviors of these faults. The length of the AA' profile across the Hsiaokangshan fault and the north segment of the Chishan fault is 35 km and its half width is 5 km. The length of the BB' profile across the south section of the Chinshan fault is 30 km and its half width is 5 km (Figure 3).

4. RESULTS

The average GPS horizontal velocity east of the Chishan fault is ~63 mm/yr, N272°. Then the velocities gradually decrease westward to 26 mm/yr, N266°. The azimuths of velocities rotate counterclockwise from EW to WSW. An obvious velocity gradient is shown between the Chishan fault and the Hsiaokangshan fault. Most the azimuths of velocities in the northern area are E-W. However, the azimuths in the southern area rotate from nearly W (~270°) to WSW (~255°) (Figure 2).

For the strain rate field, an E-W contraction with the rate of ~0.5-1.5 μstrain/yr is represented in this area (Figure 4). A nearly E-W contraction at the rate of ~1.5 μstrain/yr is shown in the northern Chishan fault; while a nearly E-W shortening at the rate of ~1.0 μstrain/yr and nearly N-S extension at the rate of ~1.0 μstrain/yr in the southern Chishan fault. In the Central Range, a remarkable extension with the rate of ~1.0-1.5 μstrain/yr is observed (Figure 4). It is worth to notice that the strain rate of ~0.5-1.0 μstrain/yr is not significant between the Hsiaokangshan fault and the Chishan fault, comparing with the values near the study area.

The distribution of rotation rates indicates clockwise rotation west of the Chishan fault. The value decreases from east to west from 25°/Myr to ~15°/Myr (Figure 5). In contrast, the counterclockwise rotation of ~5°-17°/Myr is observed between the Chishan fault and the Chaochou fault (Figure 5).

For the vertical velocity field on the northern leveling line, the vertical velocities west of the Hsiaokangshan fault is close to zero. The velocities gradually increase eastward up to ~20 mm/yr east of the Hsiaokangshan fault. Then the vertical velocities decrease eastward to the Chishan fault. For the region east of the Chishan fault, the vertical velocity is almost zero again (Figure 3). The vertical velocity field on the southern leveling line shows that no obvious uplift is represented west of Hsiaokangshan fault. However, the vertical motions increase eastward east of this fault with the maximum uplift rate of ~10 mm/yr. Then the velocities decrease westward to ~5 mm/yr east of Chishan fault. To the east, the vertical velocities decrease to zero again in the Pingtung plain (Figure 3).

Combining with the vertical velocities inferred from the data of first order first class and first order second class leveling routs from 2000 to 2008 (Ching et al.，2011) (Figure 3), the correlation between the spatial variation of vertical velocity field and the terrain elevation is shown. The uplift is represented in the hill area with the maximum uplift rate located between the Hsiaokangshan fault and the Chishan fault. The subsidence with a rate less than 10 mm/yr is shown in plain domain (Figure 3).

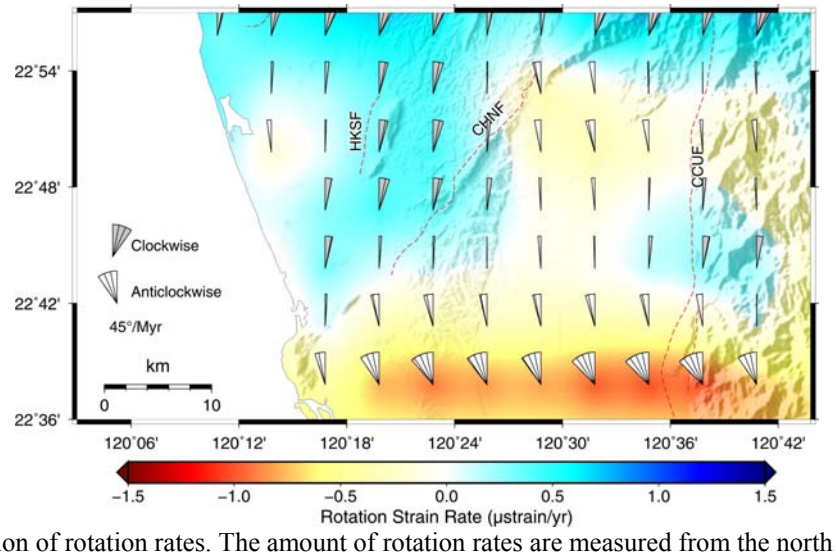

Figure 5. Distribution of rotation rates. The amount of rotation rates are measured from the north with a cone shape. Gray cone shape denotes clockwise rotation. White cone shape denotes counterclockwise rotation. The color scale represents the magnitudes of rotation rates.

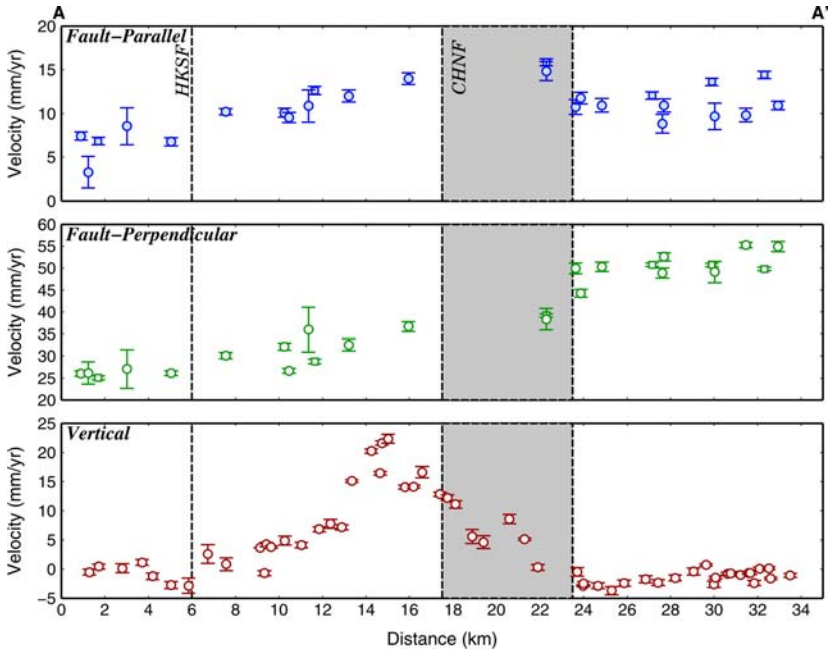

Figure 6. Velocity profile along the AA' cross-section. Horizontal velocities are decomposed into the components parallel to and normal to the strike of the Hsiaokangshan fault. Upper panels present the fault-parallel horizontal velocity components of selected stations. The central panels show the fault-normal horizontal velocity components of selected stations. The lower panels reveal the vertical velocities of selected station motions. Black dashed lines are the locations of active faults.

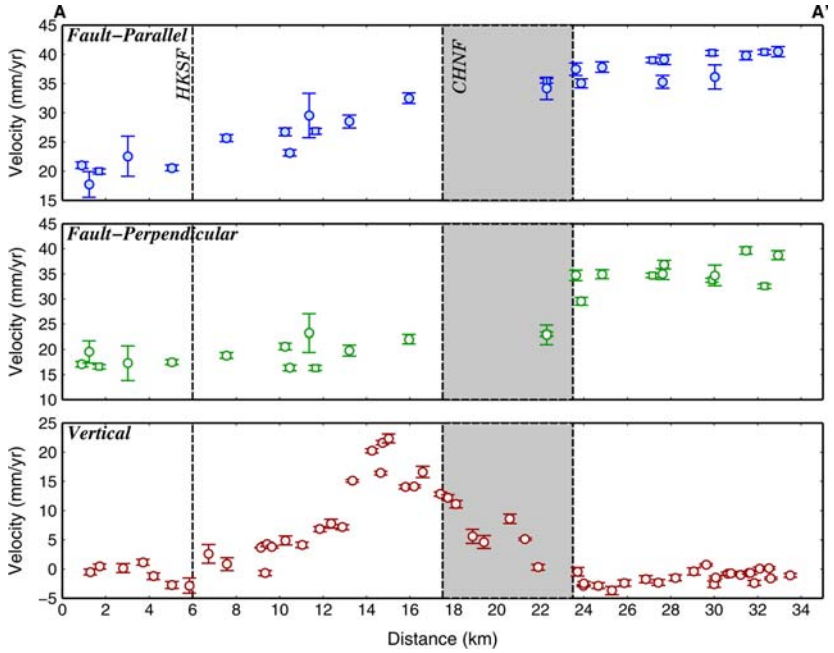

Figure 7. Velocity profile along the AA' cross-section. Horizontal velocities are decomposed into the components parallel to and normal to the strike of the Chishan fault. Upper panels present the fault-parallel horizontal velocity components of selected stations. The central panels show the fault-normal horizontal velocity components of selected stations. The lower panels reveal the vertical velocities of selected station motions. Black dashed lines are the locations of active faults.

5. CONCLUSION

Based on the spatial variation of the GPS horizontal velocities from 2002 to 2010, an obvious velocity gradient is shown between the Hsiaokangshan fault and the Chishan fault. The velocities of about ~63 mm/yr, N272° east of the Chishan fault gradually decrease westward to ~26 mm/yr, N266°, west of the Hsiaokangshan fault. According to the analysis of leveling data from 2000 to 2010, an obvious uplift is also observed in this area with the maximum uplift rate of ~20 mm/yr. However, comparing with the strain rates of nearby area, an insignificant strain rate value

of ~0.5-1.0 μstrain/yr is shown between the Hsiaokangshan fault and the Chishan fault. In addition, the distribution of rotation rate field represents clockwise east of the Chishan fault and counterclockwise west of the Chishan fault.
In terms of the GPS velocity profile analysis results, no significant velocity discontinuity is represented across the Hsiaokangshan fault. However, a notable shortening deformation with right-lateral strike-slip component between the Hsiaokangshan fault and the Chinshan fault is shown according to the velocity discrepancies of 5 mm/yr and 10 mm/yr in fault-parallel and in fault-perpendicular components, respectively, across this area. Besides, a significant shortening of ~13 mm/yr is represented across the northern segment of the Chishan fault.
According to the analyses of spatial variation of surface velocities and their velocity profiles, the major deformation belt is located between the Hsiaokangshan fault and the Chishan fault. Due to the insignificant strain rate value shown in this belt, it may imply a continuous deformation across this deformation belt or the movements of a series unpublished active faults across this belt. However, the mechanism resulted in an obvious horizontal shortening without remarkable uplift across the Chishan fault remains unclear.

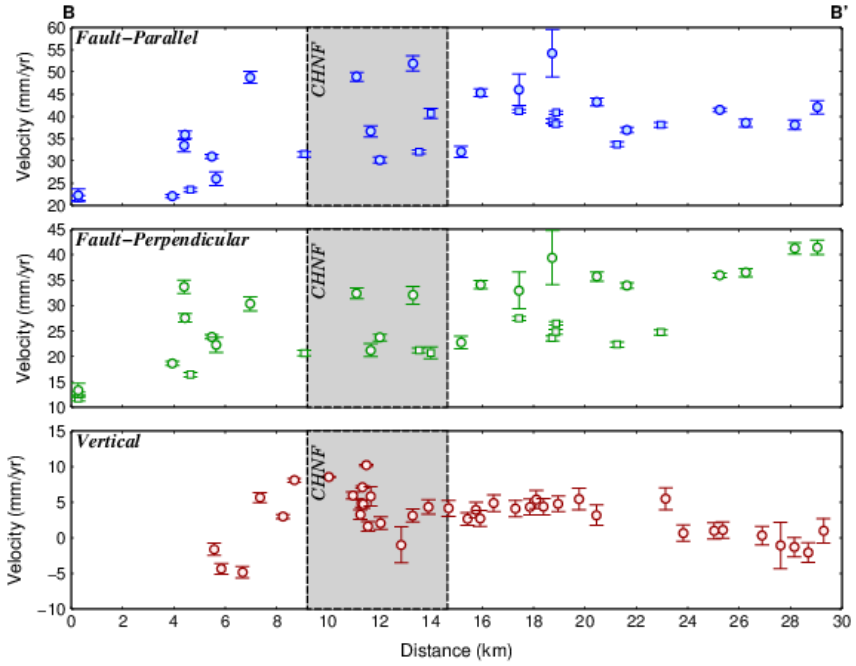

Figure 8. Velocity profile along the BB' cross-section. Horizontal velocities are decomposed into the components parallel to and normal to the strike of the Chishan fault. Upper panels present the fault-parallel horizontal velocity components of selected stations. The central panels show the fault-normal horizontal velocity components of selected stations. The lower panels reveal the vertical velocities of selected station motions. Black dashed lines are the locations of active faults.

6. REFERENCE

Bonilla, M. G., 1977, Summary of Quaternary faulting and elevation changes in Taiwan, Mem. Geol. Soc. China, 2, 43-56.

Cheng, S. N., and Y. T. Yeh, 1989, Catalog of the earthquakes in Taiwan from 1604 to 1988. Inst. Earth Sci., Academia Sinica, IES-R-661, 255pp.

Ching, K.-E., M.-L. Hsieh, K. M. Johnson, K.-H. Chen, R.-J. Rau, and M. Yang, 2011, Modern vertical deformation rates and mountain building in Taiwan from precise leveling and continuous GPS observations, 2000-2008, J. Geophys. Res., 116, B08406, doi:10.1029/2011JB008242

Huang, S.-T., K.-M. Yang, J.-H. Hung, J.-C. Wu, H.-H. Ting, W.-W. Mei, S.-H. Hsu, and M. Lee, 2004, Deformation front development at the northeast margin of the Tainan basin, Tainan–Kaohsiung area, Taiwan, Mar. Geophys. Res., 25:139–156.

Prescott, W. H., J. C. Savage, and W. T. Kinoshita, 1979, Strain accumulation rates in the western United States between 1970 and 1978, J. Geophys. Res., 84, 5423-5435.

Yu, S. B., H. Y. Chen, and L. C. Kuo, 1997, Velocity field of GPS stations in the Taiwan area, Tectonophysics, 274, 41-59.